Motion Sickness Estimation System

Chin-Teng Lin, *Fellow, IEEE*, Shu-Fang Tsai, Hua-Chin Lee, *Member, IEEE*, Hui-Lin Huang, Shinn-Ying Ho, *Member, IEEE* and Li-Wei Ko, *Member, IEEE*

***Abstract*—Motion sickness occurs when the brain receives conflicting sensory information from body, inner ear and eyes [1]. In some cases, a decreased ability to actively control the body's postural motion also causes motion sickness [2][3]. Many previous studies have indicated that motion sickness had negative effect on driving performance, and sometimes lead to serious traffic accidents due to self-control ability decline. Therefore motion sickness becomes a very important issue in our daily life especially considering driving safety. There are many attempts made by researchers to realize motion sickness, and detect motion sickness in the early stage. Although many motion-sickness-related biomarkers have been identified, estimating human motion sickness level (MSL) remains a challenge in operational environment. In our past studies, we found that features in the occipital area were highly correlated with the driver's driving performance. In this study, we designed a virtual-reality (VR) based driving environment with instinct-MSL-reporting mechanism. When a subject performed a driving task, his/her brain EEG was recorded simultaneously. From those EEG data, features associated with left motor brain area, parietal brain area and occipital midline brain area which predicted MSL were extracted by an optimal classifier implemented by an inheritable bi-objective combinatorial genetic algorithm (IBCGA) with support vector machine. Unlike traditional correlation-based method, IBCGA aims to select a small set of EEG features and maximize the prediction accuracy simultaneously in BCI applications. Once the optimal feature set predicting MSL is successfully found, a driver's cognitive state can be monitored.**

I. Introduction

Motion sickness is a common experience of numerous people. The symptoms of motion sickness are headache, sweating, disorientation, postural instability, dizziness, nausea and vomiting. About one-third of the population is highly susceptible to motion sickness, one-third experiences it in fairly rough conditions, and another third become sick only in extreme conditions [4].

C.-T. Lin and S.-F. Tsai are with the Institute of Computer Science and Engineering and Brain Research Center, National Chiao Tung University, 1001 Ta Hsueh Rd., Hsinchu 300, Taiwan.

H.-C. Lee, H.-L. Huang and S.-Y. Ho are with the Institute of Bioinformatics and Systems Biology, National Chiao Tung University, Hsinchu, Taiwan.

L.-W. Ko is with the Institute of Bioinformatics and Systems Biology and Brain Research Center, National Chiao Tung University, 1001 Ta Hsueh Rd., Hsinchu 300, Taiwan. (Correspondence author email: lwko.ece93g@gmail.com)

Of all theories on the aetiology of motion sickness, the most popular and accepted theory is the traditional sensory conflict theory posted by Reason and Brand. Their theory states that motion sickness is a self-inflicted maladaptation phenomenon, when the pattern of inputs from the vestibular system, other proprioceptors and vision is at variance with the stored patterns derived from recent transactions with the spatial environment [1].

Rapid advances in neuroimaging technology have enabled the neural correlates of motion sickness to be examined. Electroencephalography (EEG) outperforms the other technologies in its high temporal resolution and portability. The EEG studies related to motion sickness can be classified by stimuli types: vestibular stimuli and visual stimuli. Vestibular stimuli can be generated with a rotating chair, parallel swing, and cross-coupled angular stimulation, while visual stimuli can be provoked with an optokinetic drum rotating around the yaw axis. Increases of theta power in the frontal and central brain areas were reported in the previous study, when the motion sickness was induced by a parallel swing [5] and rotating drum [6],[7]; and a higher net percentage increase in EEG power in the 0.5-4 Hz band at electrode sites C3 and C4 than in the baseline spectra was found by Hu et al. when motion sickness was triggered by viewing of an optokinetic [8].

But in our daily life, motion sickness could be induced by both visual and vestibular stimuli, hence we decided to take both factors into account, and designed a virtual-reality (VR) based driving environment to simulate driving on a road with both straight and winding sections. When a subject sat in the car, he would receive not only visual but also vestibular stimulation. Our past studies [9-12] had investigated the EEG activities correlated with motion sickness in such a virtual-reality based driving simulator, and found that the parietal and motor brain regions exhibited significant alpha power suppression in response to vestibular stimuli, while the occipital area exhibited motion sickness related power augmentation in mainly theta and delta bands; the occipital midline region exhibited a broad band power increase.

In our current study, we attempt to implement an EEG-based system to estimate a subject's MSL upon the EEG power spectra from these motion sickness related brain area. This system can be applied to detect the subject's MSL even if the subject only suffers from mild motion sickness. By detecting motion sickness in the early stage, we may further prevent the various uncomfortable syndromes in the near future.

978-1-4673-1490-9/12/$31.00 ©2012 IEEE

II. MATERIALS AND METHODS

A. Experiment Design and Setup

Unlike much previous research on visual-stimuli-induced motion sickness or vestibular-stimuli-induced motion sickness, we provided both visual and vestibular stimuli in our dynamic brain research to participants to induce motion sickness through a compelling VR environment consisting of 360° projection of VR scene and a motion platform with six degree-of-freedom (shown in Fig. 1), with this environment, we might duplicate motion sickness induced in real life. During the experiment, the subjects were asked to sit inside an actual vehicle mounted on a motion platform, with their hands holding a joystick to report their sickness level continuously in real time. Furthermore, the VR scenes simulating driving in a tunnel were programmed to eliminate any possible visual distracter and shorten the depth of visual field such that motion sickness could be induced easily.

(a) Straight road

(a) Winding road

Fig. 1(a)(b) The VR environment which consists of 360° projection of VR scene

An experiment with three-section protocol (shown in Fig. 2) was designed. The first section was the baseline section which contained a 10-minute straight road to record the subjects' baseline state. The second section was a 40-minute motion-sickness section, which consisted of a long winding road, was presented to the subjects to induce motion sickness. Finally a 15-minute rest section with a straight-road condition was displayed for the subjects to recover from their sickness. The level of sickness was continuously reported by the subjects using a joystick with continuous scale on its side. The results showed that such an experimental setting could successfully induce motion sickness up to more than 80% of subjects in this study.

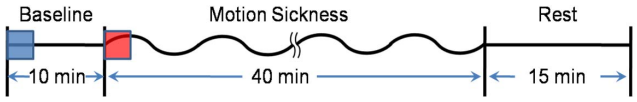

Fig. 2 A three-section experimental protocol which is comprised of baseline section, winding road section and the recovery section.

B. Subjects and EEG Acquisition

Ten healthy, right-handed volunteers with no history of gastrointestinal, cardiovascular or vestibular disorders or of drug or alcohol abuse, taking no medication and with normal or corrected-to-normal vision participated in this experiment. EEG signals were recorded with 500 Hz sampling rate by 32-channel NuAmps (BioLink Ltd., Australia). Simultaneously, during EEG recording, the level of sickness was continuously reported by each subject using a joystick with a continuous scale ranging from 0 to 5. The subjects were asked to raise/lower the scale to a higher/lower level whenever they felt more/less motion sick comparing to the last condition. Different from the traditional motion-sickness-questionnaire (MSQ) design, our mechanism allows the sickness level to be reported in real time but without interrupting the experiment.

III. SYSTEM ARCHITECTURE

Figure 3 shows the flowchart of the proposed motion-sickness-level estimation system. The idea of a MSL estimation system is to detect motion sickness in the early stage and monitor sickness level during the whole operation. However, the challenge in developing this system is to find out a set of solid indicators, i.e. a feature set, which always interpret MSL. The idea of the estimation system is composed of five function units: independent component analysis (ICA), component selection, time-frequency analysis, feature selection by an intelligent genetic algorithm, and support vector machine (SVM) classifier.

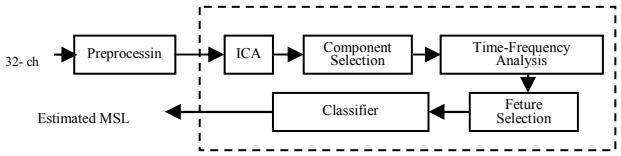

Fig. 3 System flowchart of the proposed motion sickness estimation system

A. EEG Preprocessing

The raw EEG signals were first down-sampled to 250 Hz, and then filtered with a high-pass filter and a low pass filter. A high pass filter with cut-off frequency at 1 Hz and transition band width 0.2 Hz was used to remove baseline-drifting artifacts, and a low-pass filter with cut-off frequency at 50 Hz and transition band width 7 Hz was to remove muscular artifacts and line noise. After these procedures, the preprocessed EEG signals were fed into the proposed estimation system for further analysis.

B. Independent Component Analysis

EEG recordings are usually contaminated by various artifacts including eye blinks, muscle artifact and indoor power-line noise, hence blind source separation (BSS) problem becomes an important issue to EEG based study. One of the popular methods was applying ICA to find the linear projections that maximizes the mutual independences of estimated components. This study applied ICA to separate

observed multivariate EEG signals into independent components (ICs) under the assumption of the mutual statistical independence of non-Gaussian source signals.

C. Component Selection

An equivalent current dipole model was then computed for each IC by using DIPFIT2 routines [13] from EEGLAB [14]. A four-shell spherical head model was used to compute the approximate location of each equivalent dipole source. Among components from all subjects, three components, left motor, parietal, and occipital midline, which had been proved to be highly correlated with MSL in our previous studies were selected according to their dipole location coordinates.

D. Time-frequency Analysis

Time-frequency analysis was then applied to investigate the component dynamics in frequency domain. The spectra of the components from 1 Hz to 50 Hz were calculated using 250-point non-overlapping window. In order to provide a temporal resolution of 1 second, the spectra of ICA activations were subdivided into several 125-point sub-windows and the sub-window was zero-padded to 500 points for using 500-point fast Fourier transform (FFT). The linear power spectrum density (PSD) was then converted into a logarithmic scale (dB power)

E. Feature Selection by IBCGA

Selecting a minimal number of informative EEG features while maximizing prediction accuracy of motion sickness is a bi-objective 0/1 combinatorial optimization problem. An efficient inheritable bi-objective combinatorial genetic algorithm IBCGA [15] based on an intelligent genetic algorithm IGA [16] is utilized to solve this optimization problem. IGA with an orthogonal array crossover (OAX) based on orthogonal experimental design uses a divide-and-conquer strategy and a systematic reasoning method instead of the conventional generate-and-go method to efficiently solve the combinatorial optimization problem $C(n, m)$ having a huge search space of size $n!/(m!(n-m)!)$, where n=150 (three components and 50Hz for each component) in this study. IBCGA can efficiently search the space of $C(n, r \pm 1)$ by inheriting a good solution in the space of $C(n, r)$ [33]. Therefore, IBCGA can economically obtain a complete set with various values of m for obtaining high-quality solutions in a single run.

The orthogonal experimental design utilizes properties of fractional factorial experiments to efficiently determine the best combination of factor levels. The orthogonal experimental design provides near-optimal quality characteristics for a specific objective and creates large saving in the experimental effort. The OAX randomly assigns the encoded parameters in a chromosome into α groups where each group is treated as a factor. It uses the first α columns of the orthogonal array $L_M(2^{M-1})$ and sets levels 1 and 2 of the factor d to represent the d^{th} groups of parameters coming from parents P_1 and P_2, respectively. Therefore, OAX evaluates the fitness values y_t in experiment t and the value y_1 is the fitness value of P_1. In addition, the chromosome of C_1 is formed by using the combination of the better genes from the corresponding parents, and the chromosome of C_2 is formed similarly as C_1 with the smallest main effect difference adopts the other level. Finally, the best two individuals among P_1, P_2, C_1, C_2 and M-1 combinations in the orthogonal array are used as the final children C_1 and C_2 for elitist strategy.

The chromosome encoding scheme of IGA consists of n binary genes g_i for selecting informative EEG features and two 4-bit genes for encoding γ and C of SVM parameters. The i^{th} feature (Hz) is used in the SVM classifier if g_i=1; otherwise, the i^{th} feature is excluded (g_i=0). The fitness function $f(X)$ is the prediction accuracy of selected features with the parameter settings of SVM by ten-fold cross-validation (10-CV). IBCGA can simultaneously obtain a set of solutions, X_r, where r=r_{start}, r_{start}+1, …, r_{end} in a single run. In this study, the parameter settings r_{start} =5, r_{end} =30, N_{pop} =50, p_c =0.8 and p_m =0.05. The output contains a set of m selected features and an SVM classifier with associated parameter settings γ and C. The IBCGA algorithm is given below.

Step 1: (Initiation) Randomly generate an initial population of N_{pop} individuals. All the n binary genes have r 1's and n-r 0's where $r = r_{start}$.

Step 2: (Evaluation) Evaluate the fitness values of all individuals using $f(X)$.

Step 3: (Selection) Use the traditional tournament selection that selects the winner from two randomly selected individuals to form a mating pool.

Step 4: (Crossover) Select $p_c \cdot N_{pop}$ parents from the mating pool to perform OAX on the selected pairs of parents where p_c is the crossover probability.

Step 5: (Mutation) Apply the mutation operator to the randomly selected $p_m \cdot N_{pop}$ individuals in the new population where p_m is the mutation probability. To prevent the best fitness value from deteriorating, mutation is not applied to the best individual.

Step 6: (Termination test) If the stopping condition for obtaining the solution X_r is satisfied, output the best individual as X_r. Otherwise, go to Step 2.

Step 7: (Inheritance) If $r < r_{end}$, randomly change one bit in the binary genes for each individual from 0 to 1; increase the number r by one, and go to Step 2. Otherwise, stop the algorithm.

Step 8: (System uncertainty) Perform Steps 6 and 7 for R=30 independent runs to obtain the best one of R solutions, X_m, and the associated parameter setting of the SVM classifier. The best solution can be determined by considering the accurate one S_a with the highest prediction accuracy or the robust one S_r with the highest score, where the scores S_t, t=1, …, R are derived using the following procedure Appscore.

In this study, the robust solution S_r is used. The procedure Appscore is described as the following steps:

Step 1. Calculate the appearance frequency $f(p_i)$ of each selected feature p_i from the R sets of m_t features, where i=1, …, m_t.

Step 2. Calculate score S_r for each of R solutions:

$$S_t = (\sum_{i=1}^{m_t} \mathrm{f}(p_i)) / m_t \quad (1)$$

After the optimal feature set of each subject has been identified, all the features in each feature set would be further clustered according to their frequency bands and corresponding brain areas for further analysis.

F. SVM Classifier

Support vector machine (SVM) is commonly used as an accurate and robust classifier due to its merit of generalization ability. SVM is a learning model dealing with binary classification problems. SVM constructs a binary classifier by finding a hyperplane to separate two classes with a maximal distance between margins of two classes consisting of support vectors. In order to make linear separation of samples easier, SVM uses one of various kernel functions to transform the samples into a high-dimensional search space. In this study, the radial basis function is applied to nonlinearly transform the feature space, defined as follows:

$$K(x_i, x_j) = \exp(-\gamma \left\| x_i - x_j \right\|), \gamma > 0 \quad (2)$$

The kernel parameter γ indicates how the samples are transformed into a high-dimensional search space. The penalty of total error is affected by the cost parameter C>0 of SVM. These two parameters C and γ play an important role to get the best prediction performance. In the proposed prediction method, the two parameter settings and feature selection are simultaneously optimized using IBCGA.

For the three-class classification problems, 'one-against-one' strategy is applied to transform the three-class problem into three binary classification problems. A voting strategy is applied to give a final prediction for test samples. In this study, the used SVM is obtained from LIBSVM package [17].

IV. EXPERIMENT RESULTS AND DISCUSSION

A. Experiment Results

Fig. 4 shows the training results of feature selection from Subject 1 to Subject 6. The training procedures were completed by 30 optimization trials of feature-set selection, and the highest accuracy of each Subject was chosen as the best feature set. From Fig. 5, the training accuracy of the selected feature sets from Subject 1 to Subject 6 ranges from 60% to 92%.

Fig. 5 summarizes the main effect difference (MED) score of each selected feature of Subject 1. From this figure we could see the three top-three scored features are feature 14, feature 148 and feature 1. After classification, we realized that the three features were beta band associated with left motor brain area, gamma band associated with occipital midline brain area, and delta band associated with left motor area.

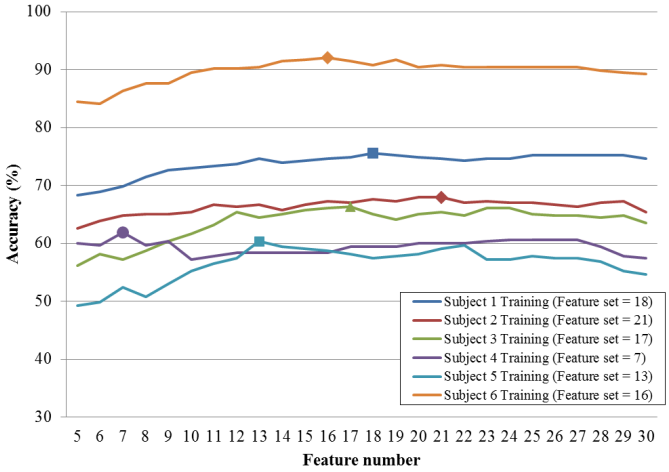

Fig. 4 The training results from Subject 1 to Subject 6.

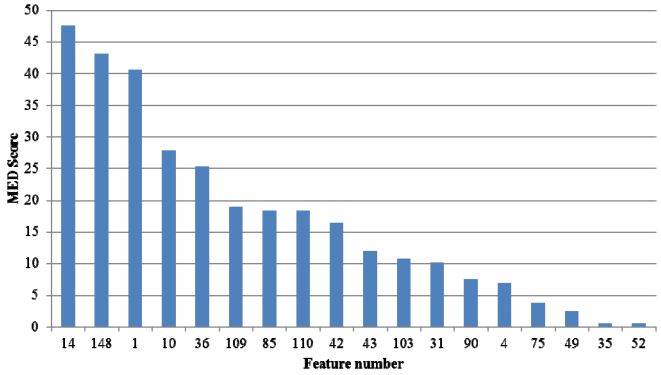

Fig. 5 The MED score of each selected feature from subject 1.

Table 1 shows the estimation accuracy of the optimal feature set of each subject. The number of features of each optimal feature set ranges from 7 to 21 and the corresponding independent test accuracy ranges from 36.3% to 73.3%.

Table 2 shows the results of feature classification. From the result of classification, we could see that features of alpha band associated with both parietal brain area and occipital midline brain area might be good indicators of MSL, besides, it is possible that gamma band features can interpret MSL very well.

Table. 1 Summary of number of features contained in the selected best feature set, and the estimation accuracy of each feature set.

Subject	S1	S2	S3	S4	S5	S6
Number of selected features	18	21	17	7	13	16
Training Accuracy	75.6%	67.9%	49.6%	61.9%	60.3%	92.1%
Test Accuracy	58.5%	59.3%	49.6%	49.6%	36.3%	73.3%

Table. 2 The results of feature classification

	Left Motor					Parietal					Occipital Midline				
	D	T	A	B	G	D	T	A	B	G	D	T	A	B	G
S1	●	●	●	●	●●●●●●	●		●		●●●	●		●		●
S2					●●●		●	●	●●	●●●●●	●			●	●●●●●●
S3				●	●●●●		●	●		●●●●			●	●	●●●●
S3				●	●			●		●	●●		●		
S5		●			●●●				●●●●	●●			●	●	●
S5	●●			●	●	●		●	●	●●	●	●	●	●●●	●

D:delta band (0.1-3 Hz) T: theta band (4-7 Hz) A: alpha band (8-12 Hz)

B:beta band (13-20Hz) G:gamma band (21-50Hz)

●: general features ●: the top-three scored features

V. CONCLUSION

It can be demonstrated that our proposed motion sickness estimation system based on EEG spectrum analysis and IBCGA is feasible, the difference between the independent training accuracy and test accuracy may have resulted from the fact that we did not smooth or moving-average the self-reported MSL as well as EEG activities, it was difficult to track the detail fluctuation of MSL. Besides, our current study shows that alpha band of brain activities may play an important role of MSL indicator, and there may be implicit information in gamma band of brain activities associated with MSL, that inspires our future work.

ACKNOWLEDGMENT

The authors would like to thank Dr. T. P. Jung, Dr. J. R. Duann, Y. C. Chen, and S. W. Chuang for their great help with developing the MS experiment paradigm, and operating the experiments and collecting the EEG data, respectively.

REFERENCES

[1] J. T. Reason and J. J. Brand, *Motion Sickness*. London: Academic press, 1975.

[2] Kohl R, Homick JL. Motion sickness: a modulatory role of the central cholinergic nervous system. Neurosci Biobehav Rev 1983; 7:73-75.

[3] Stoffregen TA, Hettinger LJ, Haas MW, et al. Postural instability and motion sickness in a fixed-based flight simulator. Humman Factors 2000; 42:458-469

[4] Murray JB. Psychophysiological aspects of motion sickness. Perceptual and Motor Skills 1997; 85:1163-1167

[5] Wood C.D., Stewart J. J., Wood M. J., Struve F. A., Straumanis J. J., Mims M. E., and Patrick G. Y.: Habituation and motion sickness, Journal of Clinical Pharmacology 34, no. 6 (1994)

[6] Wood S J.: Human otolith-ocular reflexes during off-vertical axis rotation: effect of frequency on tilt-translation ambiguity and motion sickness, Neuroscience Letters 323, no. 1 (2002)

[7] Wu J. P.: EEG Changes in Man During Motion-Sickness Induced by Parallel Swing, Space Med. Med. Eng. 5, no. 3 (1992)

[8] Hu, S., Grant, W.F., Stern, R.M., Koch, K.L., "Motion-sickness severity and physiological correlates during repeated exposures to a rotating optokinetic drum," Aviat. Space Environ.Med.62(4), pp.308-314,1991

[9] Y. C. Chen, J. R. Duann, S. W. Chuang, C. L. Lin, L. W. Ko, T. P. Jung, and C. T. Lin*, "Spatial and Temporal EEG Dynamics of Motion Sickness," *NeuroImage*, vol. 49, no. 3, pp. 2862-2870, February 2010.

[10] C. S. Wei, S. W. Chuang, W. R. Wang, L. W. Ko, T. P. Jung, and C. T. Lin, "Development of A Motion Sickness Evaluation System Based on EEG Spectrum Analysis", Proceedings of the 2011 IEEE International Symposium on Circuits and Systems (ISCAS 2011), Rio de Janeiro, Brazil, 2011

[11] C. S. Wei, S. W. Chuang, W. R. Wang, L. W. Ko, T. P. Jung, and C. T. Lin, "EEG-based Evaluation System for Motion Sickness Estimation", Proceedings of the 5th International IEEE EMBS Conference on Neural Engineering (2011)

[12] C. S. Wei, S. W. Chuang, W. R. Wang, L. W. Ko, T. P. Jung, and C. T. Lin, "Genetic Feature Selection in EEG-Based Motion Sickness Estimation", Proceedings of the International Joint Conference on Neural Network (2011)

[13] T. F. Oostendorp and R. Oostenveld, "Validating the Boundary Element Method for Forward and Inverse EEG Computations in the Presence of a Hole in the Skull." *Human Brain Mapping.* 17, 179–192,

[14] A. Delorme and S. Makeig, "EEGLAB: an open source toolbox for analysis of single-trial EEG dynamics including independent

[15] S.Y. Ho, J.H. Chen, M.H. Huang, "Inheritable genetic algorithm for biobjective 0/1 combinatorial optimization problems and its applications", *IEEE Transactions on Systems, Man, and Cybernetics, Part B: Cybernetics,* 2004, 34(1):609-620.

[16] S.Y. Ho, L.S. Shu, and J.H. Chen, "Intelligent Evolutionary Algorithms for Large Parameter Optimization Problems", *IEEE Transactions on Evolutionary Computation*, 2004. 8(6): p. 522-541.

[17] C.-C. Chang and C.-J. Lin, LIBSVM: A Library for Support Vector Machines, 2001, [Online]. Available: http://www.csie.ntu.edu.tw/~cjlin/libsvm

[18] Component analysis," *J. Neurosci. Methods*, 134, 9–21, 2004. Cheung, B., Vaitkus, P., "Perspectives of electrogastrography and motion-sickness," Brain Res. Bull. 47 (5), 421-431, 1998

[19] C-T. Lin, S-W. Chuang, Y-C. Chen, L-W. Ko, S-F. Liang, and T-P. Jung, "EEG Effects of Motion Sickness Induced in a Dynamic Virtual Reality Environment," Conference of the IEEE EMBS City International, Lyon, France, vol. 2007, pp. 3872–3875, 2007.

[20] C. T. Lin, L. W. Ko, Y. H. Lin, T. P. Jung, S. F. Liang, and L. S. Hsiao, "EEG Activities of Dynamic Stimulation in VR Driving Motion Simulator," *Lecture Notes in Artificial Intelligence,* vol. 4562, pp. 551-560, 2007.

[21] Makeig, S., Jung, T.P., Bell, A.J., Ghahremani, D.,Sejnowski, T.J., "Blind separation of auditory event-related brain responses into independent components". Proc. Natl. Acad. Sci. U. S. A. 94, pp,10979-10984, 1997.

[22] C. Jutten and J. Herault, "Blind separation of sources—part I: an adaptive algorithm based on neuromimetic architecture," Signal Processing, vol. 24, no. 1, pp. 1–10, 1991.

[23] P. Comon, "Independent component analysis: a new concept?" Signal Processing, vol. 36, no. 3, pp. 287–314, 1994.

[24] A. J. Bell and T. J. Sejnowski, "An information-maximization approach to blind separation and blind deconvolution," Neural Computation, vol. 7, no. 6, pp. 1129–1159, 1995.

[25] Bor-Chen Kuo and Kuang-Yu Chang, "Feature Extractions for Small Sample Size Classification Problem," IEEE transactions on geosciences and remote sensing, vol. 45, no. 3 March 2007, pp. 756-764, 2007.

[26] S. Makeig and M. Inlow, "Lapses in Alertness: Coherence of Fluctuations in Performance and EEG Spectrum," Electroencephalogy. Clin. Neurophysiol., Vol. 86, pp. 23-35, 1993.

[27] T. P. Jung, S. Makeig, C. Humphries, T. W. Lee, M. J. McKeown, V. Iragui, T. J. Sejnowski, "Removing electroencephalographic artifacts by blind source separation," Psychophysiology, Vol. 37, pp. 163-78, 2000.

[28] T. P. Jung, S. Makeig, W. Westerfield, J. Townsend, E. Courchesne, and T. J. Sejnowski, "Analysis and visulization of single-trial event-related potentials," Human Brain Mapping, 14(3), pp. 166-85, 2001.

[29] M. Girolami, “An alternative perspective on adaptive independent omponent analysis.”, Neural Computation, vol. 10, pp. 2103–2114, 1998.

[30] T. W. Lee, M. Girolami, and T. J. Sejnowski, “Independent component analysis using an extended infomax algorithm for mixed sub –Gaussian and super-Gaussian sources,” Neural Computation, vol. 11, pp. 606–633, 1999.

[31] K. Fukunaga, Introduction to Statistical Pattern Recognition. San Diego, CA: Academic, 1990.

[32] B.-C. Kuo and D. A. Landgrebe, “Nonparametric weighted feature extraction for classification,” *IEEE Trans. Geosci. Remote Sens.*, vol. 42, no. 5,pp. 1096–1105, May 2004.

[33] J.P. Hoffbeck and D.A. Landgrebe, “Covariance matrix estimation and classification with limited training data,” IEEE Trans. Pattern Anal. Mach. Intell., vol. 18, no. 7, pp. 763-767, July 1996.

[34] S.D. Bay, “Nearest neighbor classification from multiple feature subsets,” Intelligent Data Analysis, vol.3, no.3, pp.191-209, 1999.

[35] C-T. Lin, R-C. Wu, S-F. Liang, W-H. Chao, Y-J. Chen, and T-P. Jung, “EEG-Based Drowsiness Estimation for Safety Driving Using Independent Component Analysis,” *IEEE Trans. Circuits Syst. I, Reg. Papers*, vol. 52, no. 12, pp. 2726-2738, Dec. 2005.

[36] C. T. Lin, L. W. Ko, J. C. Chiou, J. R. Duann, R. S. Huang, T. W. Chiu, S. F. Liang, and T. P. Jung, “Noninvasive Neural Prostheses Using Mobile & Wireless EEG,” *Proceedings of the IEEE*, vol. 96, no. 7, pp. 1167-1183, 2008.

[37] C. T. Lin, I. F. Chung, L. W. Ko, Y. C. Chen, S. F. Liang, and J. R. Duann, “EEG-based Assessment of Driver Cognitive Responses in a Dynamic Virtual-Reality Driving Environment,” *IEEE Transactions on Biomedical Engineering*, vol. 54, no. 7, pp. 1349-1352, 2007.

[38] C. T. Lin, L. W. Ko, I. F. Chung, T. Y. Huang, Y. C. Chen, T. P. Jung, and S. F. Liang, “Adaptive EEG-based Alertness Estimation System by Using ICA-based Fuzzy Neural Networks,” *IEEE Transactions on Circuits and Systems I: Regular Papers*, vol. 53, No. 11, pp. 2469-2476, 2006.

[39] C. T. Lin, L. W. Ko, and T. K. Shen, “Computational Intelligent Brain Computer Interaction and Its Applications on Driving Cognition,” *IEEE Computational Intelligence Magazine*, vol. 4, no. 4, pp. 32-46, November 2009.

[40] C.-W. Hsu, C.-C. Chang, and C.-J. Lin, A Practical Guide to Support Vector Classification, 2004, [Online]. Available: http://www.csie.ntu.edu.tw/~cjlin/papers/guide/guide.pdf.